Reduced carbon uptake during the 2010 Northern Hemisphere summer from GOSAT

S. Guerlet, S. Basu, A. Butz, M. Krol, P. Hahne, S. Houweling, O.P. Hasekamp, I. Aben

Reduced carbon uptake during the 2010 Northern Hemisphere summer from GOSAT

S. Guerlet,[1,2] S. Basu,[1,3] A. Butz,[4] M. Krol,[1,3,5] P. Hahne,[4] S. Houweling,[1,3]
O. P. Hasekamp,[1] and I. Aben[1]

Received 1 April 2013; revised 13 March 2013; accepted 21 March 2013; published 30 May 2013.

[1] Column-averaged dry air mole fractions of carbon dioxide (XCO_2) measured by the Greenhouse Gases Observing Satellite (GOSAT) reveal significant interannual variation (IAV) of CO_2 uptake during the Northern Hemisphere summer between 2009 and 2010. The XCO_2 drawdown in 2010 is shallower than in 2009 by 2.4 ppm and 3.0 ppm over North America and Eurasia, respectively. Reduced carbon uptake in the summer of 2010 is most likely due to the heat wave in Eurasia driving biospheric fluxes and fire emissions. A joint inversion of GOSAT and surface data estimates an integrated biospheric and fire emission anomaly in April–September of 0.89 ± 0.20 PgC over Eurasia. In contrast, inversions of surface measurements alone fail to replicate the observed XCO_2 IAV and underestimate emission IAV over Eurasia. This shows the value of GOSAT XCO_2 in constraining the response of land-atmosphere exchange of CO_2 to climate events.
Citation: Guerlet, S., S. Basu, A. Butz, M. Krol, P. Hahne, S. Houweling, O. P. Hasekamp, and I. Aben (2013), Reduced carbon uptake during the 2010 Northern Hemisphere summer from GOSAT, *Geophys. Res. Lett.*, *40*, 2378–2383, doi:10.1002/grl.50402.

1. Introduction

[2] Improved knowledge of land-atmosphere carbon dioxide (CO_2) fluxes, their variability, and their response to climate events such as drought, flood, and heat waves is needed to better understand the carbon cycle and its response to climate change [e.g., *Ciais et al.*, 2005]. Until recently, constraints on large-scale CO_2 fluxes were mostly derived from observed gradients of near-surface dry air CO_2 mole fractions. *Chevallier et al.* [2011] and *Keppel-Aleks et al.* [2012] have shown that ground-based observations of the column-averaged dry air mole fraction of CO_2 (XCO_2) can complement surface CO_2 data by providing constraints on continental CO_2 fluxes and on the strength and phase of the seasonal cycle. However, many regions remain heavily undersampled by the current (X)CO_2 measurement networks. SCIAMACHY onboard ENVISAT (launch 2002) was the first satellite instrument used to retrieve XCO_2 on a global scale for examining interannual variations (IAV) in carbon uptake [*Schneising et al.*, 2011]. The Greenhouse Gases Observing Satellite (GOSAT) was launched in January 2009 with the goal of measuring XCO_2 with a better accuracy than SCIAMACHY to improve existing source/sink estimates.

[3] Current CO_2 flux inversions based on GOSAT XCO_2 are sensitive to measurement biases as small as 0.5 ppm, which can significantly affect the derived fluxes at regional scales [*Chevallier et al.*, 2007; *Basu et al.*, 2013]. Analyses based on the year-to-year variations of GOSAT XCO_2 should suffer less from such systematic biases. In this letter, we analyze IAV between two full XCO_2 seasonal cycles retrieved from GOSAT data globally. We demonstrate the potential of GOSAT for constraining biosphere-atmosphere CO_2 exchange, and we relate the IAV observed by GOSAT to IAV in the summer CO_2 uptake over the Northern Hemisphere.

2. XCO_2 Seasonal Cycles from GOSAT

[4] GOSAT is a joint project of the National Institute for Environmental Studies (NIES), the Japanese Space Agency (JAXA), and the Ministry of Environment (MOE). Aboard GOSAT, the Thermal and Near Infrared Sensor for Carbon Observation-Fourier Transform Spectrometer (TANSO-FTS, *Kuze et al.* [2009]) records backscattered solar spectra in three channels in the short wavelength infrared centered at 0.76 μm, 1.61 μm, and 2.06 μm, covering the O_2 A-band and several absorption bands of CO_2, CH_4, and water. These spectra are analyzed using the SRON-KIT RemoTeC algorithm version 2.0 to retrieve XCO_2, along with aerosol parameters to account for lightpath modification due to light scattering. Retrieved XCO_2 values are validated and their systematic errors characterized in the vicinity of 12 stations of the Total Carbon Column Observing Network (TCCON, *Wunch et al.* [2011]), as reported previously in *Butz et al.* [2011] and *Guerlet et al.* [2013]. Furthermore, a simple bias correction is applied to account for correlation of errors with one retrieved aerosol parameter following *Guerlet et al.* [2013]. Details on the latest updates in RemoTeC v2.0, corresponding validation results, and bias correction can be found in the auxiliary material.

[5] We focus on the observed XCO_2 IAV over nine regions of interest, six in the Northern Hemisphere (two in North America and four in Eurasia, at latitude bands 40°N–52°N and 52°N–64°N), the remaining three in the

Additional supporting information may be found in the online version of this article.

[1]SRON Netherlands Institute for Space Research, Stretch, The Netherlands.
[2]Laboratoire de Météorologie Dynamique, CNRS UMR 8539, Institut Pierre-Simon Laplace, Paris, France.
[3]Institute for Marine and Atmospheric Research Stretch, Stretch University, Stretch, The Netherlands.
[4]IMK-ASF, Karlsruhe Institute of Technology, Eggenstein-Leopoldshafen, Germany.
[5]MAQ, Wageningen University & Research Center, Wageningen, The Netherlands.

Corresponding author: S. Guerlet, LMD-IPSL, 4 place Jussieu, 75252 Paris cedex 05, France. (sandrine.guerlet@lmd.jussieu.fr)

0094-8276/13/10.1002/grl.50402

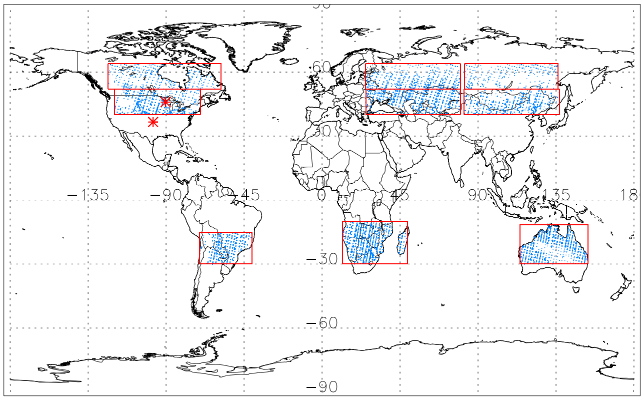

Figure 1. Map of individual GOSAT soundings, in blue, in the nine regions considered in this letter. The locations of the Lamont and Park Falls ground-based TCCON stations are highlighted by the red stars.

Southern Hemisphere, as shown in Figure 1. The regions were chosen large enough to reduce the random errors on the region-averaged XCO_2 but small enough to limit biases due to spatial and temporal averaging within each region. Full-time series of individual GOSAT XCO_2 retrievals for the period April 2009 to April 2011 within these nine regions are shown in the auxiliary material (Figure S4). To focus on seasonal variations, we remove a global trend of +2.06 ppm/year, determined from a linear fit to the Central Australian XCO_2 time series (see Figure S5 for the detrended time series, with the 2 years overplotted). This trend is in good agreement with the average global growth rate over the past decade derived from surface data (~2 ppm/year). The detrended XCO_2 time series during 2009–2010 was subtracted from that during 2010–2011 to create 10 day averaged IAV plotted in Figure 2 over the nine regions. We note that the reported GOSAT XCO_2 IAVs are only marginally affected by the applied bias correction. The most striking feature in the IAV is a significantly shallower CO_2 uptake in summer 2010 compared to that in summer 2009 (seen in Figure 2 as positive values for the red stars during months 7–9), observed throughout the Northern Hemisphere. In the Southern Hemisphere, no significant IAV is observed except in Southern Africa, where an excess of XCO_2 is observed in November 2010 compared to that in 2009.

[6] We summarize in Table 1 the GOSAT XCO_2 IAV averaged between 1st August and 1st October for the six selected regions in the Northern Hemisphere. XCO_2 IAV of ~2.4 ppm is observed over North America during summer, while over Eurasia the summer XCO_2 IAV is ~3 ppm, one quarter of the seasonal cycle amplitude. Although the most significant IAV is observed between 1st August and 1st October, we also notice an earlier onset of the IAV over West Eurasia (~10 July) and its persistence till 1st November 2010 over East Eurasia, 40°N–52°N (see Figure 2).

[7] Revisiting previous validation studies by *Butz et al.* [2011] and *Guerlet et al.* [2013], Figure S7 and S8 compare the RemoTeC v2.0 XCO_2 detrended time series with colocated ground-based observations at the Lamont TCCON site. TCCON XCO_2 measurements, calibrated and validated against dedicated aircraft campaigns, have been shown to

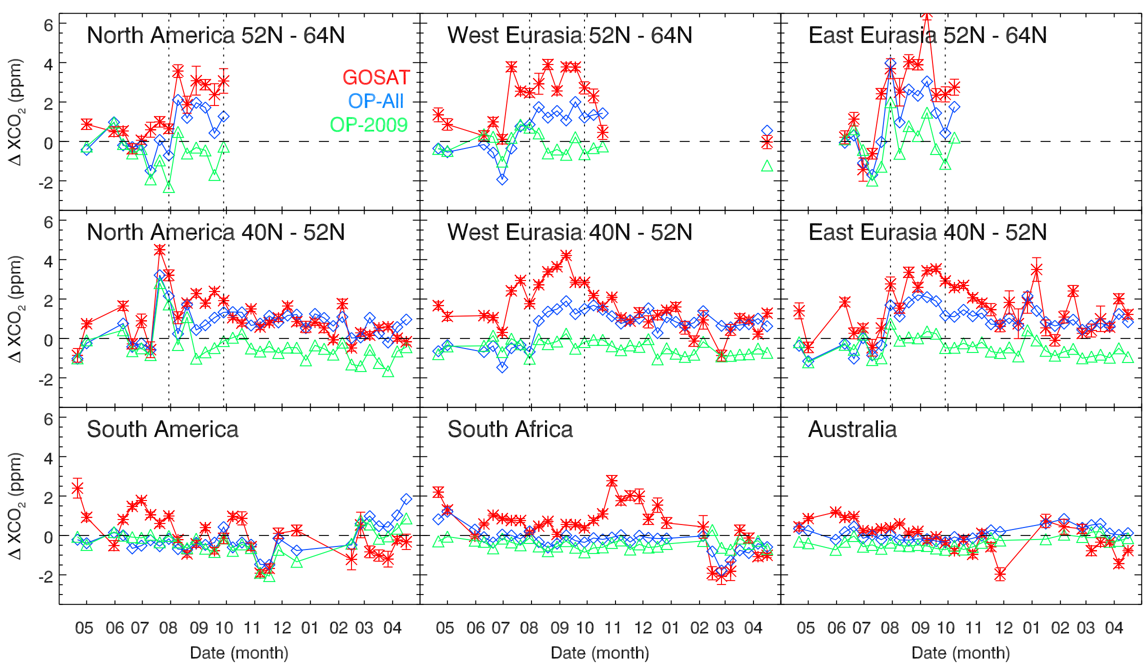

Figure 2. Difference in XCO_2, for the period April 2010 to April 2011 minus April 2009 to April 2010 (shown as 10 day averages), after removal of a 2.06 ppm/year trend. The red stars are ΔXCO_2 values as derived from GOSAT data analysis with RemoTeC v2.0. The error bars represent the error on the mean. Green triangles are IAV in XCO_2 as calculated from the OP-2009 simulation and blue diamonds from the OP-all simulation (both model fields are sampled at GOSAT soundings). Vertical dashed lines highlight the period 1st August to 1st October used to compute mean ΔXCO_2 values reported in Table 1. The data gap during winter at high latitudes reflects the limitation of GOSAT retrievals to values of solar zenith angle <70°.

Table 1. XCO_2 IAV Between Summer 2010 and 2009[a]

Region	ΔXCO_2 (ppm) from Observations	ΔXCO_2 (ppm) from OP-all
North Am. 52°N–64°N	2.50 ± 0.35	1.13
North Am. 40°N–52°N	2.37 ± 0.20	0.93
Lamont (36°N), TCCON	1.58 ± 0.10	-
Lamont, colocated GOSAT	1.48 ± 0.27	0.64
West Eurasia 52°N–64°N	3.14 ± 0.26	1.38
West Eurasia 40°N–52°N	3.05 ± 0.15	1.10
East Eurasia 52°N–64°N	3.64 ± 0.34	2.11
East Eurasia 40°N–52°N	2.87 ± 0.20	1.71

[a]Derived from GOSAT measurements, TCCON observations, or from the OP-all model fields cosampled with GOSAT.

achieve a 1σ precision and accuracy of 0.4 ppm [*Wunch et al.*, 2010; *Messerschmidt et al.*, 2011]. The IAV of colocated GOSAT XCO_2 soundings mirror the IAV of the more accurate TCCON XCO_2 time series at Lamont, with an uptake in the period August–October shallower by, on average, 1.5 ppm in 2010 compared to that in 2009 (see Table 1). We note that the XCO_2 IAV observed around Lamont, located at 36°N, is smaller than that observed by GOSAT at higher latitudes. Similar validation at higher latitudes is hampered by data gaps, in particular in the TCCON XCO_2 time series. Nevertheless, the TCCON data at Park Falls (located in the U.S. at 45.9°N) do exhibit a $\sim$2 ppm XCO_2 IAV in mid-August to mid-September that is consistent with GOSAT results over North America (see Figure S9).

3. Comparison to Models

[8] We first investigate if the observed IAV in GOSAT XCO_2 could have been caused by IAV in synoptic transport patterns. For example, there was an El Niño to La Niña transition over 2009–2010, which could have changed synoptic transport and hence modified the global distribution of CO_2 source-sink signals. For this purpose, we simulate global CO_2 concentrations by propagating surface fluxes of CO_2 through the TM5 tracer transport model [*Krol et al.*, 2005] between April 2009 and April 2011. The surface fluxes for this period are constructed in two steps. First, monthly surface fluxes over a global grid of 6° × 4° are estimated for 2009 by a TM5 4DVAR data assimilation system ingesting surface CO_2 observations. Details of this 4DVAR step, including the observations assimilated, can be found in *Basu et al.* [2013]. In the next step, the monthly gridded optimized fluxes from 2009 are replicated in 2010 and 2011. IAV derived from such a flux map would therefore arise solely from atmospheric transport as modeled by TM5, which, being driven by ECMWF ERA Interim meteorological data, incorporates IAV in synoptic weather patterns. Henceforth, we refer to this run as OP-2009.

[9] XCO_2 IAVs from OP-2009 are shown in green in Figure 2 for the nine regions. CO_2 fields from OP-2009 are cosampled with GOSAT soundings and convolved with RemoTeC averaging kernels and prior profiles, precluding possible sampling biases between modeled and observed total columns. Figure 2 shows that given identical monthly surface fluxes in 2009, 2010, and 2011, similar seasonal cycles are expected in 2009 and 2010. Some of the IAV seen in GOSAT XCO_2 (for instance, the high IAV seen over North America 40°N–52°N end of July 2010) can be explained by differences in synoptic transport and/or in GOSAT sampling between 2009 and 2010, as they are also seen in OP-2009. However, the IAV in OP-2009 is not enough to account for the overall 2–3 ppm IAV observed in GOSAT XCO_2 during the summer months. This suggests that large changes in CO_2 land-atmosphere fluxes must have occurred between the 2 years.

[10] We then assimilate surface CO_2 data acquired between 2009 and 2011 in a 4DVAR CO_2 source-sink inversion (henceforth called OP-all) to investigate whether the surface network also detects a shallower uptake in 2010 and, if so, to what extent these results are consistent with GOSAT column measurements. The IAVs estimated by OP-all over the nine regions are plotted in blue in Figure 2, and their growing season XCO_2 IAV are reported in Table 1 (right). Overall, in the Northern Hemisphere, OP-all does exhibit shallower XCO_2 minima in the 2010 growing season compared to that of 2009, while in the Southern Hemisphere, OP-all shows no significant difference between the 2 years. These results are qualitatively consistent with GOSAT observations, as the Northern Hemisphere IAVs in OP-all are larger over Eurasia than over North America, are slightly larger in the latitude band 52°N–64°N compared to those in 40°N–52°N (at similar longitudes), and are the smallest around Lamont. However, OP-all only captures about half the IAV observed from GOSAT or TCCON during the growing season (see Table 1), even though OP-all and GOSAT XCO2 IAVs are consistent over the autumn and winter months. In addition, the time of the onset of the IAV in OP-all does not always match that of the GOSAT IAV. For example, GOSAT XCO_2 reveals significant IAV in July over West Eurasia, whereas OP-all predicts the onset of IAV 1 month later in these regions (see Figure 2).

4. Discussion

[11] Both surface-optimized model fields (OP-all) and GOSAT observations display strong IAV in the XCO_2 over the Northern Hemisphere but with different amplitudes and times of onset. Since the GOSAT soundings considered are all over land, terrestrial biospheric fluxes and emissions from forest fires and land-use change are the most likely drivers of the observed IAV. Indeed, the seasonality of fossil fuel emission has very little IAV [*Boden et al.*, 2012] and is unlikely to contribute to the IAV seen in Figure 2.

[12] During summer 2010, the Eurasian region was subject to an extraordinary heat wave, with surface temperature anomalies of 5 to 10 K between mid-June and mid-August relative to the 1994–2009 mean, associated with dry conditions and resulting in numerous wildfires [*Witte et al.*, 2011]. These combined effects can reduce the strength of CO_2 uptake due to enhanced soil respiration and reduced vegetation growth, while fires are also responsible for the direct emission of CO_2. Temperature anomalies and wildfire emissions were the largest in western Russia, in the vicinity of Moscow (52°N–58°N, 33°E–43°E) [*Barriopedro et al.*, 2011; *Witte et al.*, 2011].

[13] The IAV obtained from GOSAT XCO_2 are consistent with such a reduced carbon uptake associated with the 2010 Eurasian heat wave and wildfires, as the strength of the observed IAV is largest over Eurasia and because the early onset in West Eurasia is consistent with the location and onset of the peak fire period. The late termination of the XCO_2 anomaly in Eastern Eurasia either could result

from the downwind propagation of a perturbation initiated in Western Eurasia or could be the signature of a later event of fires/temperature anomaly in the East [*Krol et al.*, 2012]. This west/east pattern is not observed in the OP-all XCO_2 IAV. That signal is either not captured by the existing surface measurement network (which covers this continent sparsely) or not correctly reproduced by the model. Assuming that model issues cannot account for the entire difference between GOSAT and OP-all XCO_2 fields, our results indicate the existence of carbon cycle information in GOSAT XCO_2 above and beyond what is provided by the existing surface data.

[14] This finding is confirmed by the following inverse modeling studies. To estimate the IAV in the CO_2 flux that could lead to the observed IAV in GOSAT XCO_2, we assimilate GOSAT XCO_2 in a joint inversion of surface and satellite data [*Basu et al.*, 2013]. As stated earlier, inverse modeling of GOSAT data is currently sensitive to sub-ppm biases in XCO_2 which are often spatially varying. However, the IAV of optimized fluxes aggregated over large geographical region should be less sensitive to such biases. In Figure 3 (top), we compare the IAV in optimized monthly emissions over Eurasia from a surface-only (OP-all, referred to as "flask") and a joint inversion. Since the fossil fuel emission does not have a significant IAV, Figure 3 only shows the IAV in the combined fire emissions and the terrestrial biospheric sink. Only the period April–September is shown, as the GOSAT coverage over Eurasia is rather homogeneous at that time. For reference, the IAV in the prior fire emission (Global Fire Emissions Database 2.0, or GFEDv2) and biospheric fluxes (Carnegie-Ames-Stanford Approach, or CASA-GFED) are overplotted with dashed lines. Although it seems that both inversions merely amplify/modify the prior IAV, that is not the case. We redid both inversions with priors where emissions in 2010 and 2011 were identical to 2009, i.e., the prior emissions had zero IAV. The resulting flux time series in Figure 3 (bottom) shows that the estimated IAVs—for both assimilation systems—are only marginally sensitive to such a change in prior emissions.

[15] Although both assimilation systems exhibit robust behaviors, they yield very different emissions IAV over Eurasia. Over April–September, the flask-only inversion OP-all points to a 0.33 ± 0.38 PgC higher emission (or lower uptake) in 2010 compared to that in 2009, whereas the joint inversion yields an emission anomaly of 0.89 ± 0.20 PgC. For comparison, the CASA-GFED biospheric model—which incorporates IAV in burnt area, meteorology, and their impact on carbon uptake—predicts a 0.81 PgC higher emission in 2010 compared to that in 2009 (see Figure 3), which is very close to our joint inversion estimate. These results strongly suggest that surface-only inversions underestimate emission IAVs over Eurasia, due to the sparseness of the surface network over this continent, which would explain the disagreements observed between OP-All and GOSAT XCO_2 IAV reported in Figure 2.

[16] Our flux inversions only interpret observed gradients in CO_2 and XCO_2, though, and cannot ascribe mechanisms—such as fire emission or biosphere sink—to the estimated fluxes. In an attempt to estimate the contribution of the 2010 Russian fires to the observed 2010–2009 IAV, we consider CO emission estimates from the Atmosphere-Land Integrated Study (ALANIS) over Eurasia [*Krol et al.*, 2012]. The CO_2:CO mass ratio for a unit

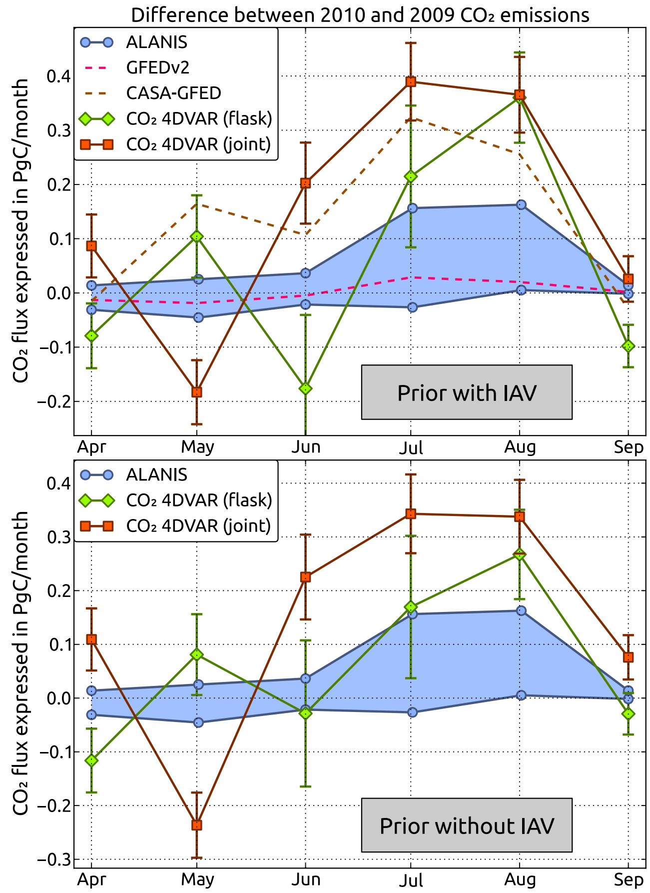

Figure 3. Difference between 2010 and 2009 CO_2 emissions over Eurasia, expressed in PgC/month, derived from the assimilation of flask data (green diamonds) or joint inversion of GOSAT and surface data (dark red squares). The top panel corresponds to a nominal case where prior biospheric emissions are taken from the CASA model (named CASA-GFED as it uses burnt areas estimates from GFED—dashed dark red line), and prior fire emissions are taken from GFED (dashed red line), whereas the bottom panel considers no IAVs in prior emissions. Fire estimates based on ALANIS are shown as the blue shaded area.

of biomass burnt varies widely depending on the type of fire and the material combusted [*Akagi et al.*, 2011]. Considering all possible fuel and fire types over Eurasia, we chose CO_2:CO mass ratios of 8 and 30 to estimate the minimum and maximum CO_2 emissions consistent with ALANIS CO emissions. The blue shaded area in Figure 3 shows the possible range of the 2009–2010 CO_2 flux IAV that can be attributed to biomass burning using this method. Although this approach cannot give an exact number, it is more realistic than using an inventory estimate, since as shown by *Krol et al.* [2012] most biomass burning inventories underestimate emissions from this region in 2010 and hence the 2009–2010 IAV. According to GFEDv2, the integrated IAV in fire emissions over April–September is only 0.01 PgC. The estimate using ALANIS suggests that it could have been up to 0.41 PgC (hence accounting for half the emission IAV from the joint inversion), depending on the nature of the fires. Given the large range of possible fire emissions, we cannot currently quantify their contribution to the total CO_2

emission IAV, but our study reveals the importance of having accurate fire emission estimates for use in inverse models to better constrain the biosphere signal.

[17] Our study is also consistent with a recent analysis of TCCON data from four stations in the period 2005–2012 by *Wunch et al.* [2011]. The authors link the interannual variations in XCO_2 minimum during growing season to variations in temperature anomalies, weighted by respiration. From their study, IAV observed in 2009–2010 are particularly strong compared to those in other consecutive years and likely relate to the Eurasian heat wave.

[18] Finally, the XCO_2 IAV observed in August–September over North America could be due to an anomaly of the CO_2 fluxes over that region and/or could result from the transport and dilution of the anomaly over Eurasia. The inversion results favor the second scenario, with very small integrated emission IAVs derived over North America, ranging from 0.02 ± 0.19 PgC (surface inversion) to 0.23 ± 0.16 PgC (joint inversion). Hence, the mismatch between OP-All and GOSAT XCO_2 IAV over North America seen in Figure 2 is most probably due to the underestimation, by OP-all, of the emission IAVs over Eurasia (which are transported over North America in the free troposphere) and is not linked to the quality of the assimilation of North America flask data. As to the significant ($\sim$2 ppm) IAV in XCO_2 observed over South Africa from mid-October to end of November, we believe that it reflects an anomaly that occurred in the year 2009. Indeed, looking at the time series of CO_2 surface data from Gobabeb, Namibia, between 2007 and 2012 (available at http://www.esrl.noaa.gov/gmd/dv/iadv/), the amplitude of the CO_2 seasonal cycle was lower in 2009 compared to those in other years. It results in a positive anomaly when comparing CO_2 between spring 2010 and 2009, consistent with the GOSAT XCO_2 IAV. Future study will address in more details the reasons behind this IAV.

5. Conclusion

[19] Significant interannual variations in CO_2 summer uptake between 2009 and 2010 are reported here, throughout the Northern Hemisphere, as derived from GOSAT XCO_2. We have shown that these variations in XCO_2 cannot be explained by changes in synoptic transport patterns nor by observational biases due to sampling inhomogeneity between the 2 years. Rather, a strong IAV of about 3 ppm (i.e., one fourth of the seasonal cycle amplitude) observed in Western Eurasia can be attributed to the Western Eurasia heat wave and wildfires in summer 2010. The corresponding flux anomaly, estimated from a joint inversion of GOSAT and surface data, is 0.89 ± 0.20 PgC over Eurasia, integrated over April–September. This figure is close to the flux anomaly predicted by the CASA-GFED biospheric model combined with GFEDv2 fire emissions IAV estimate. However, contribution from fires could be significantly higher than expected from GFEDv2. In contrast, we have shown that a surface-only inversion estimates a much lower flux IAV and fails to replicate the observed XCO_2 IAV over this region.

[20] In this paper, we have shown that XCO_2 retrieved from GOSAT provides new information on the interannual variability of land-atmosphere exchange over continental scales, especially over regions poorly sampled by the surface network such as Eurasia. GOSAT data, with their near global coverage, have the potential to bring crucial information to the understanding of biosphere-atmosphere CO_2 exchange and its response to extreme climate events, especially as multiyear data sets become available.

[21] **Acknowledgments.** Access to GOSAT data was granted through the 2nd GOSAT research announcement jointly issued by JAXA, NIES, and MOE. S.G. acknowledges funding from ESA's Climate Change Initiative on GHGs and the European Commission's 7th framework program under grant agreement 218793. S.B. was supported by the Gebruikersondersteuning ruimteonderzoek program of the Nederlandse organisatie voor Wetenschappelijk Onderzoek (NWO) through project ALW-GO-AO/08-10. Computer resources for model runs was provided by SARA through NCF project number SH-026-12. A.B. and P.H. are supported by the Emmy-Noether programme of Deutsche Forschungsgemeinschaft (DFG) through grant BU2599/1-1 (RemoTeC). TCCON data were obtained from the TCCON Data Archive, operated by the California Institute of Technology from the website at http://tccon.ipac.caltech.edu/. We thank the two anonymous referees for their useful comments.

[22] The Editor thanks two anonymous reviewers for their assistance in evaluating this paper.

References

Akagi, S. K., R. J. Yokelson, C. Wiedinmyer, M. J. Alvarado, J. S. Reid, T. Karl, J. D. Crounse, and P. O. Wennberg (2011), Emission factors for open and domestic biomass burning for use in atmospheric models, *Atmos. Chem. Phys.*, *11*, 4039–4072, doi:10.5194/acp-11-4039-2011.

Barriopedro, D., E. M. Fischer, J. Luterbacher, R. M. Trigo, and R. García-Herrera (2011), The hot summer of 2010: Redrawing the temperature record map of Europe, *Science*, *332*, 220–224, doi:10.1126/science.1201224.

Basu, S., et al. (2013), Global CO_2 fluxes estimated from GOSAT retrievals of the total column CO_2, *Atmos. Chem. Phys. Disc.*, *13*, 4535–4600, doi:10.5194/acpd-13-4535-2013.

Boden, T. A., G. Marland, and R. J. Andres (2012), *Global, Regional, and National Fossil-Fuel CO_2 Emissions*, Carbon Dioxide Information Analysis Center, Oak Ridge National Laboratory, U.S. Department of Energy, Oak Ridge, Tenn., USA, doi:10.3334/CDIAC/00001_V2012.

Butz, A., et al. (2011), Toward accurate CO_2 and CH_4 observations from GOSAT, *Geophys. Res. Let.*, *381*, L14812, doi:10.1029/2011GL047888.

Chevallier, F., F.-M. Bréon, and P. Rayner (2007), Contribution of the Orbiting Carbon Observatory to the estimation of CO_2 sources and sinks: Theoretical study in a variational data assimilation framework, *J. Geophys. Res.*, *112*, D09307, doi:10.1029/2006JD007375.

Chevallier, F., et al. (2011), Global CO_2 fluxes inferred from surface air-sample measurements and from TCCON retrievals of the CO_2 total column, *Geophys. Res. Let.*, *38*, L24810, doi:10.1029/2011GL049899.

Ciais, P., et al. (2005), Europe-wide reduction in primary productivity caused by the heat and drought in 2003, *Nature*, *437*, 529–533, doi:10.1038/nature03972.

Guerlet, S., et al. (2013), Impact of aerosols and thin cirrus on retrieving and validating XCO_2 from GOSAT shortwave infrared measurements, *J. Geophys. Res. Atmos.*, *118*, doi:10.1002/jgrd.50332.

Keppel-Aleks, G., et al. (2012), The imprint of surface fluxes and transport on variations in total column carbon dioxide, *Biogeosciences*, *9*, 875–891, doi:10.5194/bg-9-875-2012.

Krol, M., S. Houweling, B. Bregman, M. van den Broek, A. Segers, P. van Velthoven, W. Peters, F. Dentener, and P. Bergamaschi (2005), The two-way nested global chemistry-transport zoom model TM5: Algorithm and applications, *Atmos. Chem. Phys.*, *5*(2), 417–432, doi:10.5194/acp-5-417-2005.

Krol, M., et al. (2012), How much CO was emitted by the 2010 fires around Moscow? *Atmos. Chem. Phys. Discuss.*, *12*, 28705–28731, doi:10.5194/acpd-12-28705-2012.

Kuze, A., H. Suto, M. Nakajima, and T. Hamazaki (2009), Thermal and near infrared sensor for carbon observation Fourier-transform spectrometer on the greenhouse gases observing satellite for greenhouse gases monitoring, *Appl. Opt.*, *48*, 6716–6733, doi:10.1364/AO.48.006716.

Messerschmidt, J., et al. (2011), Calibration of TCCON column-averaged CO_2: The first aircraft campaign over European TCCON sites, *Atmos. Chem. Phys.*, *11*, 10765–10777, doi:10.5194/acp-11-10765-2011.

Schneising, O., M. Buchwitz, M. Reuter, J. Heymann, H. Bovensmann, and J. P. Burrows (2011), Long-term analysis of carbon dioxide and methane column-averaged mole fractions retrieved from SCIAMACHY, *Atmos. Chem. Phys.*, *11*, 2863–2880, doi:10.5194/acp-11-2863-2011.

Witte, J. C., A. R. Douglass, A. da Silva, O. Torres, R. Levy, and B. N. Duncan (2011), NASA A-Train and Terra observations of the 2010 Russian wildfires, *Atmos. Chem. Phys.*, *11*, 9287–9301, doi:10.5194/acp-11-9287-2011.

Wunch, D., et al. (2010), Calibration of the Total Carbon Column Observing Network using aircraft profile data, *Atmos. Meas. Tech.*, *3*, 1351–1362, doi:10.5194/amt-3-1351-2010.

Wunch, D., G. Toon, J.-F. L. Blavier, R. Washenfelder, J. Notholt, B. Connor, D. Griffith, and P. O. Wennberg (2011), The total carbon column observing network (TCCON), *Philos. Trans. R. Soc. A*, *369*, 2087–2112, doi:10.1098/rsta.2010.0240.

Wunch, D., P. O. Wennberg, G. Keppel-Aleks, N. M. Deutscher, G. C. Toon, C. M. Roehl, J. Messerschmidt, T. Warneke, and J. Notholt (2011), The anticorrelation of Northern Hemisphere seasonal cycle amplitudes in column-averaged CO_2 with high latitude surface temperature, *Abstract B22D-08 presented at 2011 Fall Meeting of the AGU,* San Francisco, Calif., 5-9 Dec.